

# Explainable Visual Question Answering with Multimodal Rationales

Kun Li, George Vosselman, Michael Ying Yang

**Abstract**—Visual Question Answering (VQA) is a challenging task of predicting the answer to a question about the content of an image. Prior works directly evaluate the answering models by simply calculating the accuracy of the predicted answers. However, the inner reasoning behind the prediction is disregarded in such a “black box” system, and we cannot ascertain the trustworthiness of the predictions. Even more concerning, in some cases, the models predict correct answers despite focusing on irrelevant visual regions or textual tokens. To develop an explainable and trustworthy answering system, we propose a novel model termed MRVQA (Multimodal Rationales for VQA), which provides visual and textual rationales to support its predicted answers. To measure the quality of the generated rationales, we introduce a new metric called vtS (visual-textual Similarity) score from both visual and textual perspectives. Considering the extra annotations distinct from standard VQA, MRVQA is trained and evaluated using samples synthesized from some existing datasets. The extensive experiments across four VQA datasets demonstrate that the proposed approach achieves new state-of-the-art results through additional rationale generation, enhancing the trustworthiness of explainable VQA models. The code will be released after publication.

**Index Terms**—Multimodal reasoning, Visual Question Answering, Explanations.

## I. INTRODUCTION

VISUAL Question Answering (VQA) takes as input an image and a natural language query and predicts the corresponding answer based on the understanding of the provided vision-language content. It is more challenging than other fundamental computer vision tasks (e.g., object detection [1]), since it requires fusion and reasoning cross different modalities. With the rapid developments of deep neural networks, recent approaches [2]–[5] achieve promising performance on VQA. Normally, the answer accuracy is employed in most VQA systems to measure the correctness of the predictions. However, the users cannot know how reliable the predicted answers are, purely based on the accuracy number. In contrast, explainable VQA (EVQA) tries to link the predicted answer to the given image-question pair by providing explanations in different formats (e.g., image regions of interest, and textual explanations) to support the answering process simultaneously. This explanatory mechanism enables VQA systems to reason for complex multimodal information fusion and scene understanding.

Significant progress has been made in the field of “explainable artificial intelligence” (XAI) [6], with remarkable

success in uncovering the inner workings of AI algorithms and providing insights into how they arrive at their decisions. However, there remains a largely unexplored area in developing human-centric explanations for interactive vision-language tasks, such as VQA. Most of the prevailing methods adopt single-track models to improve the explainability: either visual hints (termed “V-Exp”) or textual explanations (termed “T-Exp”), as illustrated in Fig. 1 (b). V-Exp methods [7], [8] predict the answer to the given image-question pair and further extract the regions of interest by analyzing the heat maps or attention maps in the inner neural network layers. However, the provided information is usually coarse and inaccurate while the image regions of interest are restricted to a region level, which is not human-friendly for understanding the decision-making process. T-Exp methods [9]–[11] aim to describe the visual content of the image that helps explaining the answer in natural language. The explanation partially reproduces the reasoning process behind answering the question. However, it still lacks a rich comprehension of the vision-language input when we aim to directly and visually identify the specific target (i.e., the zebra in the green bounding box from Fig. 1 (d)). Another drawback arises from the inconvenience of textual explanations in complex scenes (e.g., multiple zebras lying on the ground or the presence of horses), leading to longer and more detailed descriptions of the relevant objects. Based on the above concerns in mind, we observe that the current single-track EVQA methods cannot satisfy the credibility of an interactive vision-language system.

In fact, prior to this paper, a few works have made significant strides towards EVQA with compositional reasoning. However, these works essentially provide various relationships among present objects with external information (e.g., scene graphs [12]), resulting in a lack of visual recognition capabilities (as shown in Fig. 1 (c)). Specifically, the textual explanations are either chosen from multiple choices or generated using functional programs from a predefined candidate pool. The shortcuts within the external information allow the model to directly utilize these relationships (e.g., spatial relation and object category), which can harm the model’s general performance. In addition, the external information itself is expensive to collect. To our knowledge, few previous studies have explored free-form textual explanations alongside precise visual predictions.

Moreover, the assessment of generated explanation quality remains limited to basic text similarity measures. The existing methods [8], [9], [13] for EVQA employ widely-used metrics for text generation evaluation, such as BLEU [14], ROUGE [15], and CIDEr [16]. Normally, these metrics quantitatively

Kun Li and George Vosselman are with the Faculty of ITC, University of Twente, the Netherlands (k.li@utwente.nl; george.vosselman@utwente.nl).

Michael Ying Yang is with the Visual Computing Group, Department of Computer Science, University of Bath, UK (myy35@bath.ac.uk).

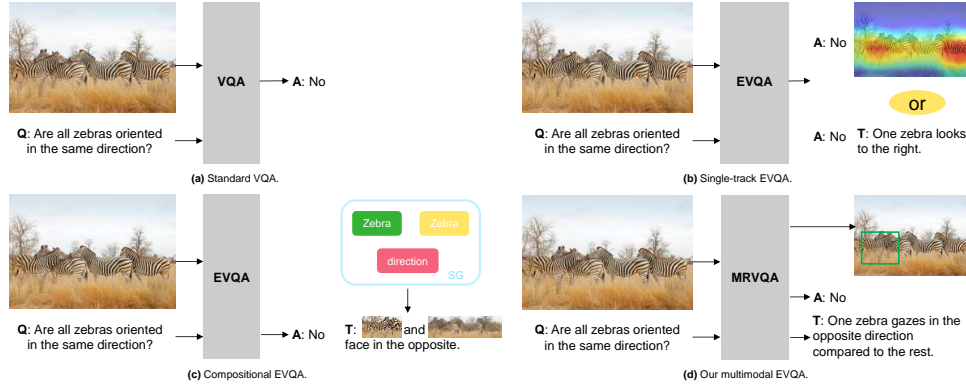


Fig. 1. Illustration of the differences between standard VQA, single-track EVQA, compositional EVQA and our multimodal EVQA. Our model answers the question and simultaneously predicts textual and visual rationales to support the answer.

compare the generated text to reference texts from various textual aspects (*e.g.*, n-gram overlap, semantic similarity, word order, and structure), while ignoring the role of visual content in cross-modality tasks. However, an ideal evaluation of multimodal explanations should consider both visual and linguistic perspectives. Unfortunately, neither the qualitative evaluation of attention maps nor the correspondence score between detected bounding boxes and referred expressions effectively enhances the explainability and credibility of VQA.

Therefore, in this work, we attempt to address these problems and move towards a multimodal EVQA task. Specifically, we propose a new model called **MRVQA** (Multimodal Rationale for Visual Question Answering) that not only predicts accurate answers but also delivers both textual and visual rationales. To highlight the differences between existing EVQA methods and our approach, we present an example in Fig. 1. Compared to single-track ones, our approach can simultaneously provide multimodal rationales, offering more reliable and user-friendly explanations. For instance, the textual rationale “One zebra gazes in the opposite direction” and the visual rationale, represented by the green bounding box, complement each other to support the answer prediction “no”. Different from compositional ones, our approach generates free-form textual rationales and precise bounding boxes without relying on external information. From a data perspective, we synthesize a multimodal rationale dataset by augmenting existing datasets to alleviate the annotation effort required by EVQA. From a model perspective, we base our approach on a Transformer architecture [17], projecting features into the latent space of a large language model for textual predictions, and fusing features to extract bounding boxes by leveraging a pre-trained open-vocabulary detector. Additionally, we propose a loss function designed to promote the effective cross-alignment and balance among multitask predictions. From an evaluation perspective, we introduce a new metric, which incorporates both visual and textual views to assess the generated rationales and advance EVQA research.

The **main contributions** of this paper are summarized as follows:

- We introduce **MRVQA**, a new EVQA model that facilitates the system to provide multimodal explanations for answer predictions through textual and visual rationale

generation. Moreover, a new loss is introduced to balance multitask predictions and generate reasonable rationales.

- To assess the quality of generated rationales, we introduce a new metric called **vtS** for evaluating natural language from a visual perspective. We employ both textual similarity and the visual presence of key objects to enhance the comprehensive evaluation of the explainability.
- We demonstrate the effectiveness of our model with extensive experiments under different settings. The proposed model achieves superior performance over the existing methods on both single-track and multimodal EVQA datasets.

## II. RELATED WORK

### A. Visual Question Answering

Visual Question Answering (VQA) has been defined as the task of providing an answer to a question based on the context of an image. As a fundamental and challenging task in the vision-language field, VQA requires cross-modality understanding and reasoning. Traditionally, it is considered as a classification problem with a pre-defined answer candidate pool and later expanded to free-form open-ended answering. As this task takes as input both images and questions, VQA models address the problem through diverse approaches in different stages, including feature extraction [2], alignment [18], fusion [19], and prediction [20]. With the rapid development of Transformers [17], both natural language processing and computer vision communities have witnessed remarkable advances in vision-language tasks [21], [22]. For instance, MCAN [23] introduced a deep modular co-attention network by leveraging intra-modal self-attentions and cross-modal guided attentions, which enhanced the feature representation and alignment. Some recent works [24], [25] investigate leveraging the vision-language pre-training from large-scale data to enhance the efficacy of VQA models and enable complex reasoning, pioneering the burgeoning trend in the vision-language community. These methods rely on extensive pre-training data and meticulous fine-tuning for downstream tasks, yet they still infer answers through a “black-box” system, which diminishes the explainability of results. In contrast, we utilize multimodal rationales to support answer predictions and enhance model credibility.

### B. Explanations for VQA

Deep neural networks are typically “black-box” systems because their internal mechanics and decision-making processes are not easily interpretable or understandable. Some pioneering works have emerged that bring explanations to VQA. Visualization is the first idea adopted to display the inherent details of models, aiding users in understanding the predictions. For instance, VQA-HAT [7] collected human attention maps of where humans choose to look so as to answer questions, visually providing coarse explanations for VQA. Textual explanations utilize natural language to articulate the reasoning behind the system’s predictions. VQA-X [8] combined textual explanations annotated by humans and visual pointing (similar to attention maps) to construct a multimodal reasoning dataset. Subsequently, Li et al. [9] further emphasized textual explanations by employing a semi-automatic construction method using caption annotations, creating a large-scale EVQA dataset (*i.e.*, VQA-E). VCR [26] transferred the generation task to a simpler classification one by building a multiple choice movie-scene dataset. GQA-REX [13] constructed a large-scale visually grounded textual explanation dataset by extending the previous GQA [27] dataset with an automatic scheme. However, the displayed decision-making process heavily relies on the pre-defined functional programs with external information (*e.g.*, scene graphs and correlations), which reduces its applicability in a diverse open world. Chen et al. introduced a visually grounding dataset VizWiz-VQA-Grounding [28] with questions asked by people with visual impairments. Although the queried objects were annotated with boundaries, the questions lack both in quantity and complexity, and there are no accompanying explanations for the corresponding answers. Differently, we synthesize an EVQA dataset by augmenting existing datasets and provide multimodal explanations through free-form texts and precise bounding boxes.

### C. Generating Multimodal Explanations

The increasing interest in understanding the reasoning behind VQA has led to the development of various methods across both textual and visual perspectives [13], [26]. Park et al. [8] first adopted an LSTM [29] to generate textual explanations and subsequently displayed the internal visual focus through attention maps. Li et al. [9] employed two prediction heads to generate answers and textual explanations, respectively. Wu et al. [10] proposed to leverage the consistency between gradient-based visual explanations and answers to generate robust textual explanations. These earlier works employ encoders to separately extract intra-modality features, which are then simply fused being passed to the final prediction stage. Marasović et al. [30] incorporated pretrained language models with object recognition, visual semantics, and scene graphs to generate textual explanations. Dua et al. [3] introduced a network comprising a generation module and a refinement module, both utilizing sequential LSTMs for answer and explanation generation. DMRFNet [11] leveraged pre-trained semantic relation embeddings and adaptively fused spatial and semantic features through multi-

graph reasoning and fusion layers. REX [13] enhanced cross-modality alignment by considering the semantic similarity between words and image regions. Subsequently, VCIN [31] extended relationships to include words, image regions, and explanation tokens through a gating transformer with variational causal inference. However, these methods restrict the relations with pre-defined compositions (*e.g.*, semantic relations, scene graphs and functional programs). In addition, visual explanations are usually generated through gradient-based segmentation proposals [10] or post-processed visual regions [13], [31]. Different from the aforementioned methods, our proposed approach focuses on generating free-form textual explanations and object-level visual explanations.

### D. Grounding with Text

Referring expression comprehension, also known as visual grounding [32], [33], is a task of locating the targets conditioned on the provided natural language expression. Existing models can be categorized into two groups: two-stage methods [34] first generate region proposals and then select the best matching results while one-stage methods [35] directly predict the detected results. For instance, Grounding-DINO [1] concatenated all category names into a single input text, encoded to a text embedding, and then output the top-k highest scores for object detection. However, these visual grounding models rely on specific and direct text inputs (*e.g.*, category) to identify target objects, whereas the input questions may not always provide this information. For example, when posed with the question “which one is taller in the park?”, the aforementioned methods might struggle to accurately extract the relevant objects. In this work, we address this problem by generating textual rationales that explain the predictions by detailing the involved targets. It is worth mentioning that we have conducted an ablation in Section IV-C to analyze the impact of linguistic inputs.

## III. METHOD

### A. Problem Formulation

We first revisit the standard VQA setting. Given an image  $I$  and a natural language question  $Q$ , the desired output of a VQA model is an answer  $A$  (*i.e.*, a single word or a short phrase) that relates the queried image. As reviewed in Section II-A, standard VQA methods provide direct answers but lack explainability and credibility.

To overcome the limitation in standard VQA, we expand the model’s predictions beyond a single answer to include multimodal rationales, offering explanations from both visual and textual perspectives. Regarding the textual part, we follow previous single-track EVQA methods [9], [11] and employ a similar text description to explain the related context for answering the question, which we refer to as the textual rationale  $TR$ . In contrast to previous methods [8], [36] that use region-level attention maps for visual explanations, we utilize precise bounding boxes of relevant objects as the visual rationale  $VR$ . This setting directly links the question and answer through clear and object-specific visual information. To this end, given  $I$  and  $Q$ , the goal of our multimodal EVQA

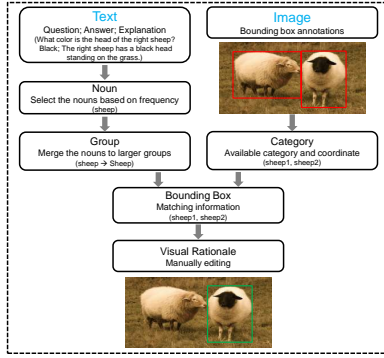


Fig. 2. The overall process of the multimodal EVQA dataset synthesis. The text in the brackets shows an example.

model is to predict multiple results: (1) an answer  $A$ ; (2) a textual rationale  $TR$ ; and (3) a visual rationale  $VR$ . It is simply formulated as follows,

$$\{A, TR, VR\} = P(I, Q; \theta), \quad (1)$$

where  $\theta$  represents the parameters of an EVQA model. With the support of both visual and textual rationales, users can easily understand the logical context behind the answering and see the visual correspondence, as displayed in Fig. 1 (d). It is particularly valuable for users who wish to explore more details in an interactive scenario. Moreover, these rationales enhance the model’s explainability and credibility.

### B. Multimodal EVQA Dataset Synthesis

To perform the multimodal EVQA task, we review the available EVQA datasets [7]–[9], [13], [26] as discussed in Section II-B. Unfortunately, we have observed that these datasets lack either precise visual evidences or related textual descriptions. To avoid the labor-intensive process of annotating explanation-aware VQA examples, we propose a semi-automatic approach to synthesize examples by augmenting an existing EVQA dataset. We select the VQA-E [9] dataset for its comprehensive set of examples that include detailed textual explanations and, importantly, for its integration with the COCO dataset [37] that provides precise bounding-box annotations for object detection. Briefly, we complement the visual explanations by incorporating these annotations. We begin by aligning potential annotations with samples from the VQA-E dataset based on shared objects. Subsequently, we manually refine these results to ensure the dataset quality.

Figure 2 illustrates the overall process involved in synthesizing the multimodal EVQA dataset. Specifically, we first extract all nouns from the question-answer-text triplets in the VQA-E dataset. These nouns usually identify the objects relevant to the explanation of answer predictions. For instance, given a question “What color is the tie of that boy?”, the visual focus of the explanation corresponds to the objects “tie” and “boy”. However, analyzing all nouns is impractical due to the presence of over 10K categories. To address this, we conduct a frequency analysis of the nouns, selecting those that appear more than 20 times. This step yields 1,247 distinct nouns that can be matched with the visual labels. Unfortunately, COCO only includes annotations

TABLE I  
STATISTICS FOR THE COMPARISON BETWEEN THE SYNTHESIZED EVQA DATASET AND PRIOR DATASETS. BOUNDING BOX AND SCENE GRAPH ARE ABBREVIATED AS B-BOX AND S-G, RESPECTIVELY.

Dataset	Image	#Image	#Q&A	#TR	#VR	VR Format
VQA-HAT [7]	COCO	20K	59K	-	62K	Region
VQA-X [8]	COCO	28K	32K	41K	6K	Region
VQA-E [9]	COCO	108K	269K	269K	-	-
VCR [26]	Movies	99K	264K	264K	-	-
Vizwiz-G [28]	Phone	9K	9K	-	9K	Boundary
GQA-REX [13]	GQA	82K	1040K	1040K	82K	S-G
VQA-E-Syn	COCO	20,367	33,726	33,726	93,377	B-box

for 80 object categories. To address this, we implement a strategy that classifies candidate nouns into broader categories aligned with the existing COCO annotations. For instance, nouns like “man”, “woman”, “people”, “boy”, and “girl” are categorized under the “Person” category in COCO. However, not all bounding boxes within a given category are relevant for explanations of a specific image-question pair. For example, in Fig. 2, only one sheep is applicable as the visual rationale for the question about the “right sheep”, despite two sheep present. Additionally, the extracted objects from nouns may not fully capture the logical context of the answering process. For instance, with a question “What is the man doing?” where the answer is “surfing” and the text is “a man on the wave” we can only extract the bounding box for the noun “man”. Ideally, the visual rationale should encompass both “man” and “surfboard”. To ensure the accuracy and relevance of visual rationales, we manually refine the bounding boxes by removing irrelevant objects and incorporating additional objects that are essential for the explanations. This process results in the synthesis of a dataset, including image-question pairs annotated with answers, textual rationales, and visual rationales, thereby facilitating multimodal EVQA.

We further analyze the synthesized multimodal EVQA dataset (VQA-E-Syn) and compare it with available datasets in Table I. Overall, the dataset comprises 33,726 question-answer pairs derived from 20,367 images, adhering to the original split in the VQA-E dataset. Each pair is accompanied by a textual rationale and an average of 2.8 bounding boxes for visual rationales. The distinctions from previous EVQA datasets are highlighted in the last three columns (*i.e.*, the quantity and format of multimodal rationales). For instance, in comparison to the VQA-X dataset [8], our VQA-E-Syn dataset provides more comprehensive and precise visual rationales. We believe this synthesized dataset will foster future research in multimodal EVQA, which will be made publicly available.

### C. Multimodal EVQA Network

The overall framework of the proposed MRVQA model is shown in Fig. 3. Since our intention is to establish a simple and computation-friendly baseline model for the multimodal EVQA task, we have designed a model to be clean and adaptable to various scenarios. Here, we introduce the core components of our approach: input representation, encoder-decoder architecture, projection module, predictors, and loss functions.

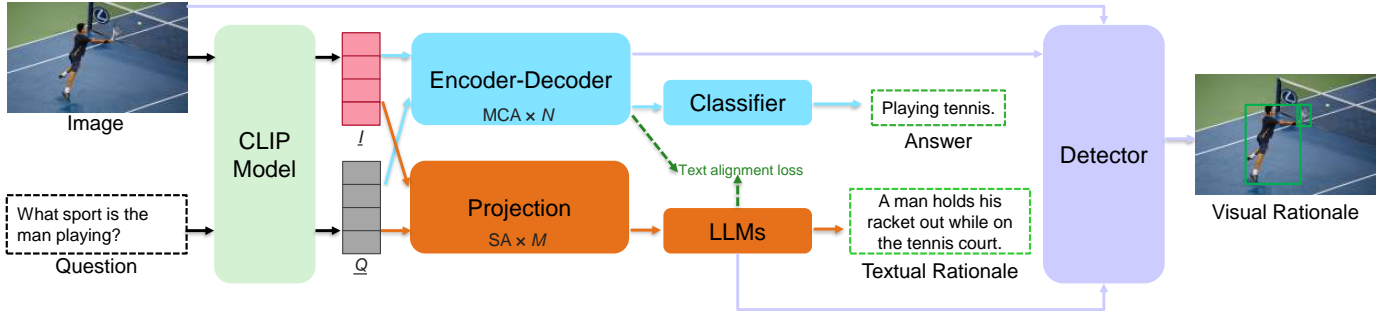


Fig. 3. The framework of the proposed MRVQA model. The notations  $\underline{I}$  and  $\underline{Q}$  represent the pre-trained CLIP [38] features for the image and the question, respectively. The proposed text alignment loss helps to improve the coherence of text predictions.

1) *Input Representation*: Different from previous methods that use separate visual and linguistic feature extractors, we utilize a pre-trained vision-language model (*i.e.*, CLIP [38]) to simultaneously represent both the input image and question. The CLIP model, pre-trained on large-scale image-caption pairs and benefited from transferable representations, outperforms intra-encoders trained solely on in-domain data. To support the cross-modal understanding required for VQA, we employ the pre-trained CLIP model that leverages powerful encoders (*e.g.*, ViT [39] and Transformers [17]), which enhance robust feature extraction and offer promising scalability.

2) *Encoder-Decoder*: To effectively understand the queried focus from the visual and linguistic features, it is essential to exploit cross-modality fusion for VQA tasks. To enhance representations without introducing a new backbone or altering the model’s structure, we build on the popular VQA baseline MCAN [23], which cascades several Modular Co-Attention (MCA) layers. The MCA layer comprises self-attention units and guided-attention units. The former capture intra-modal features, while the latter enable cross-modal interactions. We employ the default structure and parameters in MCAN-base to build a simple and clean model for our EVQA task.

3) *Projection Module*: Large language models (LLMs) have been employed to generate sequential texts in our approach. However, there is a gap between pre-trained representations and LLMs in multimodal tasks. To alleviate the mismatch between different feature spaces, a projection module is often employed to facilitate better adaptation and integration. A straightforward linear projection is widely adopted and has proven effective. To strengthen the connection between pre-trained CLIP features and LLMs, we propose a Transformer-based [17] projection module. The self-attention mechanism enables the learning of global dependencies between tokens, even within the context of long sentences. Inspired by Darce et al. [40], we introduce two additional tokens as learnable constants for the CLIP features  $\underline{I}$  and  $\underline{Q}$ , respectively. These constant tokens act as registers, allowing the model to store and retrieve meaningful information efficiently. For the entire projection module, we utilize eight self-attention layers to process the dual-stream visual and linguistic features. The projected features  $I_{proj}$  and  $Q_{proj}$  are calculated as follows,

$$I_{proj} = SA(Cat(\underline{I}, C)), Q_{proj} = SA(Cat(\underline{Q}, C)), \quad (2)$$

$$SA(q, K, V) = Softmax\left(\frac{qK}{\sqrt{d}}\right)V, \quad (3)$$

where  $C$  represents the learnable constants,  $q$ ,  $K$ ,  $V$  and  $d$  denote query, Key, Value, and dimensionality of values, respectively. We fuse the projected features  $I_{proj}$  and  $Q_{proj}$  by concatenating before feeding the results  $f_{proj}$  into the LLMs.

4) *Predictors*: Since the multimodal EVQA task encompasses generating answers, textual rationales, and visual rationales, we utilize different predictors in our model. For the answer prediction, we approach it as a classification problem, similar to previous methods [2], [19]. Specifically, we utilize a linear fusion module, followed by a sigmoid function, to process the cross-attended features from the decoder. For textual rationales, in contrast to earlier methods that rely on simple LSTMs [29], we utilize advanced LLMs to generate more robust and relevant textual rationales. However, given the complexity of handling multiple tasks in EVQA, the LLMs integrated into the model should facilitate computationally efficient fine-tuning for multimodal learning. To address this, we leverage the auto-regressive large language model GPT-2 [41]. For each token in the sequence, GPT-2, conditioned on the projected features  $f_{proj}$ , generates probability distributions over the entire vocabulary. These distributions are then used to predict the next token in the sequence, enabling the generation of complete textual rationales. For visual rationales, we generate precise object-level bounding boxes using Grounding-DINO [1], an open-vocabulary object detector capable of identifying arbitrary objects based on natural language inputs. In contrast to the original work, our approach inputs the detector with the image  $I$ , cross-attended features  $f_{cross}$ , and LLM-processed features  $f_{llm}$ . In addition, we set all detected bounding boxes as a single category, diverging from standard visual grounding practices [32]. This setting addresses the challenge of aligning objects with the input question when specific descriptions are absent. For example, when given the phrase “a red baseball bat”, visual grounding models can effectively match the object “bat” to the relevant image regions. However, for a question like “What color is the object?”, the models might struggle to discern the category information from the image-question pair due to the lack of explicit context. With the incorporation of various predictors, our model provides robust results for multimodal EVQA through an end-to-end supervised mode.

5) *Loss Functions*: During model training, we use full supervision with annotated examples to generate answers, textual rationales, and bounding boxes. A hybrid loss function is employed to refine the model, with different loss components



tailored for each type of prediction in our EVQA task. For the answer prediction, we use a sigmoid function to output a score  $\hat{s}$  ranging from 0 to 1, representing the probability of the answer. Consistent with previous methods [9], we employ the widely-used binary cross-entropy loss [42] as  $L_{ans}$  to supervise these predictions. To train the model for generating textual rationales from the LLM-processed features  $f_{ilm}$ , we utilize the simple yet effective cross-entropy loss as  $L_{tr}$  in our case. Given  $M$  questions,  $N$  candidate answers,  $M$  textual rationales,  $L_{ans}$  and  $L_{tr}$  are calculated as follows,

$$L_{ans} = - \sum_i^M \sum_j^N s_{ij} \log(\hat{s}_{ij}) - (1 - s_{ij}) \log(1 - \hat{s}_{ij}), \quad (4)$$

$$L_{tr} = - \sum_i^M \sum_t^l \log p_\theta(w_t^i | f_{ilm}^i, w_1^i, \dots, w_{t-1}^i), \quad (5)$$

where  $l$  and  $\theta$  represent the maximum length of tokens and the model's trainable parameters, respectively. The sequenced tokens are denoted as  $w^i = w_1^i, \dots, w_l^i$ . For visual rationale generation, we directly adopt the existing loss function from Grounding-DINO [1], including L1 loss, GIoU loss, and contrastive loss. We combine them together as our vision objective  $L_{vr}$  for brevity. To train the entire model using multi-task learning, we take a linear combination of the different loss components as follows,

$$L_{base} = L_{ans} + L_{tr} + L_{vr}, \quad (6)$$

where  $L_{base}$  denotes the base objective of our multimodal EVQA task. Note that we remove the final component of  $L_{base}$  for our MRVQA-C model due to the lack of visual supervision from the annotations.

Moreover, to improve the coherence between answers and their corresponding textual rationales, we introduce a new loss function termed **text alignment loss** (abbreviated as  $L_{ta}$ ). Specifically, the improvement of text coherence is achieved by the alignment between cross-attended features  $f_{cross}$  and LLM-processed features  $f_{ilm}$ . We use the cosine similarity function to measure the feature similarity between these dual objectives from the textual side. The text alignment loss  $L_{ta}$  is obtained as follows,

$$L_{ta} = 1 - \sum_i^M \sum_t^l \cos(f_{ilm}^{ti}, f_{cross}^{ti}), \quad (7)$$

where  $f_{cross}'$  and  $f_{ilm}'$  represent the co-matched features in a common vector space through two MLP layers. Before incorporating it into the final loss function, we use a trade-off parameter  $\lambda$  to balance the basic and alignment components of the loss. The overall loss  $L$  of the model is defined as follows,

$$L = L_{base} + \lambda L_{ta}, \quad (8)$$

Compared to previous single-track and compositional EVQA methods [9], [13], our proposed loss function ensures greater consistency between answer prediction and textual rationale generation, avoiding the disconnection often seen with multiple predictors. In addition, the visual rationale generation leverages features from both the answer and text spaces, contributing to a unified model.

#### D. Visual-Textual Similarity Score

Previous methods for text generation tasks (e.g., translation and retrieval) commonly utilize word-level or phrase-level similarity evaluation metrics, such as BLEU [14], ROUGE [15] and SPICE [43], to evaluate model performance. However, these metrics primarily capture low-level aspects (e.g., fluency and coherence), while overlooking the high-level interactions between sentences that do not strictly match word-for-word. Fortunately, the similarity score between sentence embeddings is a good option to measure the quality of generated texts. We utilize the powerful pre-trained text embedding model, GTE [44], to map the generated textual rationales for similarity comparison. There are several reasons for selecting this model: (1) The GTE model employs contrastive learning across a diverse range of datasets, which allows it to generalize effectively to various data; (2) It avoids the reliance on prompt formulation seen in LLMs; (3) It handles pairs of short and long texts more effectively without requiring word-level alignments, which is ideal for comparing our generated free-form texts; (4) It outperforms previous embedding methods in comprehensive benchmarks [44]. We believe the GTE model is well-suited to measure the similarity between the generated textual rationales and the ground truth. Specifically, we use the cosine function to assess textual similarity. To handle the negative values produced by the cosine function, we map the cosine similarity scores to a range from 0 to 1. The textual similarity ( $TS$ ) is calculated as follows,

$$TS = \frac{1 + \cos(\text{GTE}(T_{pred}), \text{GTE}(GT))}{2}, \quad (9)$$

where  $T_{pred}$  and  $GT$  represent the generated textual rationale and the ground truth, respectively. For visual evaluation, we assess the predicted bounding boxes by calculating the Average Precision [45] (AP) in comparison to ground truths.

For a unified multimodal model, it is essential to evaluate its performance from both visual and textual perspectives, ensuring coherence across different predictions. However, simply averaging  $TS$  and  $AP$  scores fails to fully capture the model's performance, particularly when one modality significantly lags behind the other in certain scenarios (e.g., occlusion or ambiguity). To address this, we introduce a new metric **vtS** (visual-textual Similarity score), which combines visual evaluation and textual similarity to provide a balanced assessment of the quality of the generated multimodal rationales. The metric **vtS** is defined as follows,

$$vtS = \frac{2 \times TS \times AP}{TS + AP}, \quad (10)$$

Given the interdependence between visual and textual rationales, more detailed and relevant texts can improve the extraction of bounding boxes. Likewise, more accurate visual rationales help guide the generation of more focused and precise textual descriptions. The combined evaluation metric provides a unified way to assess overall model performance.

### IV. EXPERIMENTS

#### A. Experiment Setup

1) *Datasets*: We conduct the primary experiments on the synthesized multimodal EVQA dataset (VQA-E-Syn) intro-

TABLE II

COMPARISON RESULTS ON VQA-E-SYN REGARDING TEXTUAL RATIONALE GENERATION. ALL NUMBERS ARE REPORTED IN PERCENTAGE (%). THE BEST RESULTS ARE **BOLD** WHILE THE SECOND BEST ARE UNDERLINED.

Method	Image Feature	Question Feature	Text Predictor	BLEU-4	METEOR	ROUGE	CIDEr	SPICE	vtS
PJ-X [8]	CNN	LSTM	LSTM	8.78	16.94	35.65	89.31	15.32	49.19
VQA-E [9]	CNN	GRU	LSTM	8.93	17.02	35.96	90.84	16.83	51.88
FME [10]	CNN	GRU	LSTM	12.81	21.26	37.69	89.16	18.77	53.82
CCM [47]	CNN	LSTM	LSTM	8.85	17.86	38.42	92.46	18.35	54.44
DMRFNet [11]	CNN	GRU	GRU	13.34	19.44	40.76	95.68	20.41	56.06
REX [13]	VilBert	VilBert	LSTM	14.71	21.35	41.86	100.75	21.08	56.38
OFA [48]	CNN	BPE	Seq2Seq	<u>16.38</u>	22.09	42.74	103.25	22.65	56.58
VCIN [31]	V-Bert	V-Bert	Trans	15.77	22.38	43.10	104.63	22.07	57.89
MRVQA-TR	CLIP	CLIP	GPT2	15.08	21.77	42.04	102.86	21.22	57.30
MRVQA-C	CLIP	CLIP	GPT2	15.84	<u>22.41</u>	<u>43.57</u>	<u>105.31</u>	22.19	<u>58.19</u>
MRVQA-E	CLIP	CLIP	GPT2	<b>16.97</b>	<b>23.02</b>	<b>44.28</b>	<b>107.04</b>	<b>23.68</b>	<b>59.16</b>

duced in Section III-B. In addition, we evaluate models on three existing VQA datasets, including VQA-X [8], GQA-REX [13], and VQAv2 [46], to access the its adaptability and generalization capability under different settings.

2) *Training and Inference Settings*: Under full supervision using the synthesized dataset, we refine the MRVQA model in an end-to-end manner, referred to as MRVQA-E. The proposed loss function is designed to help optimize the training process, enhancing the model’s ability to generate both answers and multimodal rationales. To adapt to various practical scenarios, we simplify the MRVQA model to predict the required results under different conditions. For example, we develop a variant, MRVQA-C (combined), by removing the visual generator component, allowing us to test the model’s ability to generalize in the absence of visual rationale supervision. This variant utilizes the generated textual rationales and the input images to guide the Grounding-DINO [1] model in predicting bounding boxes during inference stage. In addition, we further simplify the MRVQA model to focus exclusively on answer prediction or textual rationale prediction, developing variants called MRVQA-A and MRVQA-TR for direct comparison with previous standard VQA methods and single-track EVQA methods, respectively. Note that only the relevant loss functions are utilized for these simplified models.

3) *Implementation Details*: We utilize the pre-trained CLIP model [38] with ViT-base [39] and Transformer [17] architectures for visual and linguistic feature representation. The cross-attended and LLM-processed features are provided as additional inputs to the feature enhancer of the Grounding-DINO-T model. We use the AdamW [49] optimizer with the learning rate of  $2 \times 10^{-5}$ . All the models are trained for 50 epochs with a batch size of 64 using two A40 GPUs, within a consistent PyTorch environment. To ensure a fair comparison, we follow the official repositories of the relevant methods and reimplemented all the models on the synthesized dataset.

4) *Evaluation Metrics*: For VQA evaluation, we maintain consistency with prior works by using answer accuracy as the metric. To evaluate generated textual rationales, we employ five mainstream metrics, namely BLEU-4 [14], METEOR [50], ROUGE [15], CIDEr [16] and SPICE [43] (B, M, R, C, S for their abbreviations, respectively), which measures the linguistic similarity between the generated text and the ground truth. Additionally, we use the newly introduced metric **vtS** to better capture the cross-modality similarity by leveraging

the visual response. The widely-used Average Precision (AP) metric [45] is employed to assess the quality of the generated bounding boxes by comparing them to ground truths.

### B. Comparisons with the State-of-the-Art Methods

1) *Results on the synthesized VQA-E-Syn*: Table II reports the comparison with the state-of-the-art EVQA methods on the synthesized VQA-E-Syn dataset. Our proposed MRVQA-E model significantly enhances the generation of textual rationales for multimodal EVQA, outperforming the previous methods. The achieved higher scores on the evaluation metrics demonstrate that our generated text excels in fluency, relevance, and accuracy. For example, our approach achieves a 2.41% improvement in CIDEr compared to VCIN [31], highlighting its superior fluency and coherence. For evaluating multimodal rationales, we report results using the introduced vtS. It is worth mentioning that we employ a combined approach similar to our MRVQA-C variant to gather visual predictions for comparison with the previous methods that do not support that. The results demonstrate that our approach achieves a 1.27% improvement over VCIN in vtS. To ensure a fair comparison, we also evaluate our MRVQA-TR and MRVQA-C models. Both variants demonstrate slightly superior performance compared to the previous methods. More importantly, the comparison between the end-to-end model and its variants highlights that incorporating visual rationale generation improves linguistic prediction performance.

Table III shows the results compared to the state-of-the-art VQA methods on VQA-E-Syn in terms of answer accuracy. The methods listed in the top section are trained solely for answer prediction, whereas those in the middle section have the capability to generate both answers and textual explanations. For example, MCAN [23], LXMERT [51], and UNITER [52] are popular models for standard VQA. OFA [48], as a powerful unified sequence-to-sequence framework, facilitates generating multiple predictions through separate fine-tuning processes on task-specific datasets (*e.g.*, VQA and image captioning). To adapt OFA for our EVQA task, generating texts within a unified inference pass, we perform a single fine-tuning of the OFA-base model on the combined samples from VQA-E-Syn. Our MRVQA-E model achieves an overall accuracy of 75.01% and an average accuracy of 72.46% on VQA-E-Syn, surpassing the previous methods. Notably, the model shows

TABLE III  
COMPARISON RESULTS ON VQA-E-SYN REGARDING ANSWER ACCURACY. OA AND AA REPRESENT OVERALL AND AVERAGE ACCURACY, RESPECTIVELY.

Method	Number	Yes/No	Other	OA	AA
MUTAN [19]	49.23	65.52	60.27	61.07	58.34
BUTD [2]	52.68	64.07	65.72	64.13	60.83
MCAN [23]	59.19	71.70	72.37	71.09	67.76
LXMERT [51]	59.93	72.34	73.04	71.76	68.44
UNITER [52]	61.58	73.81	72.66	72.14	69.35
BLIP [4]	63.68	72.43	74.83	73.16	70.31
CMQEF [53]	60.02	71.63	72.20	71.03	67.95
VQA-E [9]	54.26	63.98	66.45	64.67	61.57
DMRFNet [11]	59.08	72.28	73.84	72.15	68.40
REX [13]	59.73	72.91	74.18	72.84	68.94
OFA-base [48]	60.48	73.26	75.37	73.49	69.70
VCIN [31]	61.59	73.47	73.10	72.43	69.39
MRVQA-A	57.02	72.80	73.41	71.89	67.75
MRVQA-C	63.20	76.03	75.72	74.81	71.65
MRVQA-E	<b>65.11</b>	<b>76.40</b>	<b>75.87</b>	<b>75.01</b>	<b>72.46</b>

TABLE IV  
COMPARISON RESULTS ON VQA-X [8] AND GQA-REX [13] FOR ANSWER AND TEXTUAL RATIONALE EVALUATION.

Dataset	Method	B	M	R	C	S	OA
VQA-X	PJ-X [8]	19.5	18.2	43.7	71.3	15.1	-
	VQA-E [9]	20.7	18.6	44.2	75.6	15.6	70.2
	FME [10]	24.4	19.5	47.4	88.8	17.9	-
	CCM [47]	21.1	19.7	44.9	73.9	16.2	-
	DMRFNet [11]	20.5	19.9	41.3	74.5	17.6	72.6
	VCIN [31]	25.9	21.6	48.5	93.7	<b>19.4</b>	77.7
	MRVQA-C	<b>26.6</b>	<b>22.0</b>	<b>48.9</b>	<b>98.4</b>	19.2	<b>78.8</b>
GQA-REX	VQA-E [9]	42.56	34.51	73.59	358.20	40.39	57.24
	FME [10]	42.45	34.46	73.51	357.10	40.35	56.92
	REX [13]	54.59	39.22	78.56	464.20	46.80	57.77
	VCIN [31]	58.65	41.57	81.45	519.23	54.63	60.61
	MRVQA-C	<b>58.83</b>	<b>42.01</b>	<b>83.07</b>	<b>528.42</b>	<b>54.96</b>	<b>61.28</b>

significant improvements in the *Number* and *Yes/No* question categories, with increases of 1.43% and 2.59%, respectively. Similarly, comparing MRVQA-E with its variants (last three rows) reveals that incorporating additional rationale supervision enhances the performance of the answering process. This approach provides more detailed information, significantly benefiting the VQA model.

2) *Results on VQA-X*: Table IV reports the results compared to previous EVQA methods on VQA-X [8]. As VQA-X only supports linguistic examples (shown in Table I), to ensure a fair comparison, we conduct experiments with MRVQA-C for only answer and textual rationale generation. Our approach achieves a 78.8% overall accuracy, which is higher than the previous state-of-the-art VCIN by 1.1%. The comparison of the generated textual explanations across various metrics also demonstrates that our approach surpasses previous methods. For instance, the model shows significant improvements in BLEU-4 and CIDEr metrics, with increases of 0.7% and 4.7%, respectively, compared to VCIN.

3) *Results on GQA-REX*: Table IV also shows the results on GQA-REX [13]. Note that the previous VCIN model predicted region-level patches and compared results with other adapted methods using the Grounding metric [13], which relied on priors in visual encodings (e.g., patch location). Due to the single-category object detection used in our settings, we exclude this unfair comparison and only report the textual

TABLE V  
RESULTS ON VQAv2 [46] TEST-DEV REGARDING ANSWER ACCURACY. 129M\* AND 9M\* SAMPLES ARE STATED IN [52] AND [4]. THE TOP SECTION LISTS METHODS TRAINED (☉) OR FINE-TUNED (✓) ON VQAv2, WHILE THE BOTTOM INCLUDES METHODS (✗) WITHOUT THESE STEPS.

Method	Training Dataset	Data Scale	Fine-tuned?	OA
BUTD [2]	VQAv2	443K	☉	65.3
VQA-E [9]	VQAv2	443K	☉	66.2
MCAN [23]	VQAv2	443K	☉	70.6
UNITER [52]	Combined	9M*	✓	73.8
BLIP [4]	Multiple	129M*	✓	<b>78.3</b>
VQA-E [9]	VQA-E	181K	✗	62.5
DMRFNet [11]	VQA-E	181K	✗	62.9
BLIP2 [54]	Multiple	129M*	✗	65.0
MRVQA-E	VQA-E-Syn	23K	✗	<b>66.8</b>

results. Our approach achieves an overall answer accuracy of 61.28%, representing a 0.67% improvement over the previous state-of-the-art VCIN. Meanwhile, our model maintains competitive performance even without external information (e.g., functional program and scene graph), achieving 58.83% and 83.07% for BLEU-4 and ROUGE scores, respectively. These results highlight the model’s strong generalization capability across different datasets.

4) *Results on VQAv2*: We further assess our model’s transfer learning capabilities on VQAv2 [46] and compare the results with previous methods in Table V. The top section of the table displays methods that were either trained from scratch or pre-trained on large-scale datasets before being fine-tuned on VQAv2. As expected, results improve with the use of more powerful models and larger datasets. For example, BLIP [4], which is pre-trained on over 129 million image-text pairs, achieves 78.3% accuracy after thorough fine-tuning on VQAv2. The methods listed in the lower section of the table are trained on alternative datasets without subsequent fine-tuning, allowing us to assess the robustness and generalization capability of these models. For example, we directly evaluate our pre-trained MRVQA-E model on VQAv2. Despite being trained on relatively limited data (23K) compared to other methods, our approach achieves competitive performance, reaching 66.8% accuracy on a standard VQA task. The comparison with BLIP2 [54] highlights the effectiveness of integrating rationales into the answering system.

### C. Ablation Studies

1) *Ablation of the Projection Module*: In the proposed MRVQA model, we introduce a Transformer-based projection module to map the pre-trained CLIP features to the latent space of LLMs. For comparison, we conduct an ablation study by replacing the projection module in MRVQA-E with a linear layer, as used in prior vision-language methods. The results in Table VI show that our Transformer-based projection module significantly enhances the performance of textual rationale generation compared to the linear layer across various metrics. For example, the incorporation of our module results in a 5.46% improvement in CIDEr score. Additionally, the enhancement in linguistic predictions contributes to a 2.02% increase in the multimodal rationale evaluation metric vtS, highlighting the efficacy of our proposed module.



TABLE VI

ABLATION RESULTS OF USING DIFFERENT PROJECTION MODULES FOR MULTIMODAL RATIONALE GENERATION ON VQA-E-SYN.

Module	B	M	R	C	S	vtS
Linear [55]	15.07	22.13	42.74	101.58	22.06	57.14
Ours-Transformer	<b>16.97</b>	<b>23.02</b>	<b>44.28</b>	<b>107.04</b>	<b>23.68</b>	<b>59.16</b>

TABLE VII

ABLATION RESULTS OF DIFFERENT STRATEGIES FOR TEXT PREDICTIONS ON VQA-E-SYN.

Strategy	Data	B	S	OA	AA
Generator	{A + TR}	15.16	20.98	70.42	68.39
Classifier + Generator	{A, TR}	<b>15.84</b>	<b>22.19</b>	<b>74.81</b>	<b>71.65</b>

2) *Ablation of Unified or Separate Text Predictor:* For text predictions, we utilize two separate predictors: a classifier for answer prediction and a generator for textual rationale prediction. This approach is designed to ensure high accuracy in answer predictions with a concise format (*i.e.*, short and straightforward), making the results more accessible to non-expert users. Additionally, this separation avoids the need for redundant task-specific fine-tuning, as seen in previous pre-training methods [48], [52]. Some approaches [54] use a unified strategy for all text-related downstream tasks, which often results in longer and more complex expressions. To compare it with our approach, we adapt the unified strategy by integrating answer prediction into the text generation process, using samples in {answer, textual rationale} format (*e.g.*, “the boy because only the boy can catch the frisbee”). Since the primary focus of this ablation is on the text prediction, we use the MRVQA-C model to ensure a fair comparison. Table VII reports the performance of different text prediction strategies. As expected, while the performance of textual rationale generation shows only a slight change, the overall accuracy significantly drops by 4.39%, indicating a decrease in the robustness of an answering model. Consequently, we employ dual-head predictors for linguistic output to address this issue in our EVQA task.

3) *Ablation of the Text Generator:* In our proposed approach, we use GPT-2 as the textual rationale generator. To evaluate its effectiveness compared to commonly used text generation models, such as LSTMs and Transformer, we replace this component in MRVQA-E with these alternative modules. The results are shown in Table VIII. Comparing the first three rows, GPT-2 significantly outperforms standard LSTMs and yields slightly better results than Transformer, even with frozen parameters. This comparison proves the similar observation on the effectiveness of the powerful pre-training in Table V. Subsequently, we allow the parameters of GPT-2 to be trainable within our MRVQA-E model to boost generation performance. While this requires additional effort to train the LLMs, it enhances the quality of the generated textual rationales. For instance, it results in a 13.78% improvement in the CIDEr score. This advancement in linguistic understanding also positively impacts visual predictions, as evidenced by a 5.82% increase in the vtS score. We further replace the text generator with the more advanced GPT-3 model [56], known for its superior performance in complex

TABLE VIII

ABLATION RESULTS OF DIFFERENT TEXT GENERATORS UNDER EITHER FREEZING OR FINE-TUNING SETTINGS ON VQA-E-SYN.

Generator	Mode	B	M	R	C	S	vtS
LSTM [29]	-	12.65	18.39	36.77	88.82	18.45	53.14
Transformer [17]	-	12.89	18.91	37.03	89.14	18.86	53.17
GPT-2 [41]	freezing	13.27	20.08	38.33	93.26	19.25	53.34
GPT-3 [56]	freezing	15.06	21.27	39.74	98.90	20.57	56.25
MRVQA-E	fine-tuning	<b>16.97</b>	<b>23.02</b>	<b>44.28</b>	<b>107.04</b>	<b>23.68</b>	<b>59.16</b>

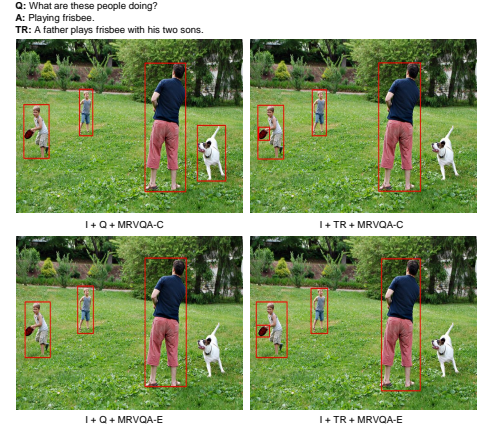


Fig. 4. Examples of generated visual rationales (bounding boxes in red) with different linguistic inputs for our MRVQA-C and MRVQA-E models.

reasoning and contextual understanding. However, GPT-3’s size (175 billion parameters compared to GPT-2’s 1.5 billion) poses significant challenges, and moreover, it is not available for fine-tuning. Given our intention to fine-tune LLMs for easy adaptation and computational efficiency, we utilize GPT-3 with frozen parameters for generating textual rationales. The results indicate that using more advanced LLMs does not significantly impact the performance of text generation for our EVQA task.

#### 4) Ablation of Linguistic Features for Vision Predictor:

To assess the impact of linguistic features on the vision predictor Grounding-DINO, we perform experiments on VQA-E-Syn using features derived from either questions or textual rationales as input. We observe that the variant using features from input questions struggles (41.93% AP), as these do not provide comprehensive and clear referring information like visual grounding [57]. In contrast, features derived from textual rationales significantly enhance the detection model, leading to 47.45% AP (a 5.52% improvement) in the MRVQA-E model. In addition, Fig. 4 shows a qualitative comparison between the variant and our approach using both MRVQA-E and MRVQA-C models. The results demonstrate that our proposed approach leverages the generation of textual rationales to significantly enhance performance for multimodal EVQA.

5) *Ablation of Loss Functions:* To further evaluate the proposed loss function, we conduct ablation experiments on VQA-E-Syn to verify its effectiveness. The results are reported in Table IX. Comparing the first two rows, we can see that incorporating visual supervision significantly improves overall performance across all types of predictions, which is consistent with our earlier observations in Table II and Table III. Comparing the last four rows, we observe a notable enhancement in performance due to the inclusion of our proposed

TABLE IX  
ABLATION RESULTS OF LOSS FUNCTIONS ON VQA-E-SYN.

$Loss_A$	$Loss_{TR}$	$Loss_{VR}$	$Loss_{TA}$	B	S	vtS	OA
✓	✓			15.84	22.19	-	71.65
✓	✓	✓		15.13	22.34	59.01	72.28
✓	✓	✓	$\lambda = 0.1$	16.49	23.51	59.10	74.76
✓	✓	✓	$\lambda = 0.5$	<b>16.97</b>	<b>23.68</b>	<b>59.16</b>	<b>75.01</b>
✓	✓	✓	$\lambda = 1$	16.25	23.40	59.07	74.59

TABLE X  
ABLATION RESULTS OF THE MULTIMODAL EVALUATION METRIC ON VQA-E-SYN.

Method	S	TS	AP	(1)	(2)	(3)
PJ-X [8]	15.32	68.32	38.43	53.38	26.26	49.19
VQA-E [9]	16.83	71.67	40.65	56.16	29.13	51.88
FME [10]	18.77	73.16	42.57	57.87	31.14	53.82
DMRFNet [11]	20.41	75.06	44.74	59.90	33.58	56.06
VCIN [31]	22.07	78.13	45.97	62.05	35.92	57.89
MRVQA-C	22.19	<b>79.57</b>	45.86	62.72	36.49	58.19
MRVQA-E	<b>23.68</b>	78.56	<b>47.45</b>	<b>63.00</b>	<b>37.28</b>	<b>59.16</b>

text alignment loss. For example, all configurations utilizing  $Loss_{TA}$  show at least a 1% improvement in SPICE scores over the others. In addition, we perform a series of experiments to determine the optimal value for the trade-off parameter  $\lambda$ . The results from the last three rows indicate that setting  $\lambda = 0.5$  yields the best performance. This suggests that the balance component is relatively less important than the basic loss components for achieving the multimodal predictions.

6) *Ablation of the New Metric*: To verify whether the introduced metric vtS effectively measures the quality of the generated multimodal rationales, we perform a series of analyses in this part. Table X reports the results. We begin by evaluating the textual similarity score (TS) derived from the GTE [44] model. The results in the first two columns show that the quality of textual rationales, as represented by TS, aligns well with the SPICE metric. Additionally, we explore various combinations of visual and textual aspects in the multimodal rationale evaluation. Specifically, we consider three options: (1) averaging AP and TS by taking their mean; (2) multiplying AP and TS; (3) dividing the result from (2) by the result from (1), which we refer to as vtS. We observe that options (1) and (2) fail to accurately reflect model performance when there is a significant discrepancy between the two components (e.g., comparing VCIN and MRVQA-C, and considering that visual predictions would deteriorate further if the model’s performance were to decline). In contrast, option (3) mitigates the impact of large discrepancies, offering a more balanced assessment (e.g., 0.3% with (3) compared to more than 0.7% with (1)). Consequently, we use the combination approach outlined in (3) as the new evaluation metric vtS for our multimodal EVQA task.

#### D. Qualitative Analysis

We conduct a qualitative analysis of predicted answers and rationales. Fig. 5 displays three examples from the synthesized multimodal dataset VQA-E-Syn. Compared to the previous methods such as DMRFNet [11] and VCIN [31], our proposed approach demonstrates superior performance in both answer-

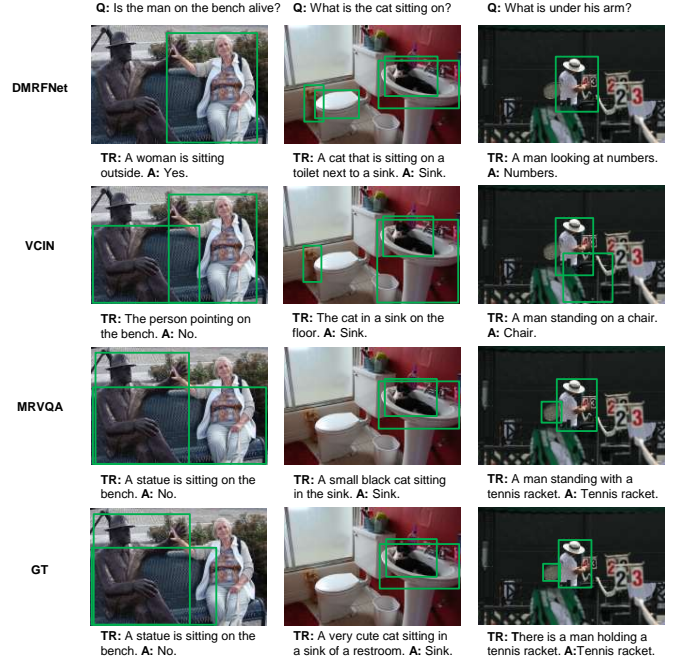


Fig. 5. Qualitative results of our approach compared to the previous methods. The bounding boxes in green display the relevant visual rationales.

ing and rationale support. For example, in the first column, both DMRFNet and VCIN struggle to comprehend the query’s intent, misleading them to focus on the object “woman,” although VCIN ultimately predicts the correct answer “No”. In contrast, our MRVQA model effectively performs cross-modal understanding, accurately identifying the target “man” referring to the statue and correctly predicting the answer, accompanied by reasonable rationales. Another example in the second column illustrates our model’s ability to capture relevant objects in both visual and textual rationales. Our MRVQA model successfully identifies the action “sitting on” and accurately locates the target, while the other methods are misled by “the other cat” or “the toilet”. Additionally, the final example demonstrates our EVQA model’s reasoning capability. Despite the lack of category-level information, the model accurately predicts the answer and delivers consistent multimodal rationales, as evidenced by the references to “the man” and “the tennis racket”. These examples demonstrate that our approach not only delivers accurate answers but also offers robust and reliable multimodal rationales, effectively explaining the prediction process.

#### V. DISCUSSION AND LIMITATIONS

While our approach has shown advancements through extensive experiments across various datasets, there remain several areas for further exploration in future research. In our proposed model, we utilize the pre-trained CLIP model to represent input questions and images. However, the model may encounter problems when users’ focus is on local details within images or when contextual information is limited. We show two failure cases in Fig. 6 to illustrate these problems. In the left example, our model predicts the wrong answer and fails to identify the relevant objects due to the challenge of distinguishing the target among numerous similar objects. This

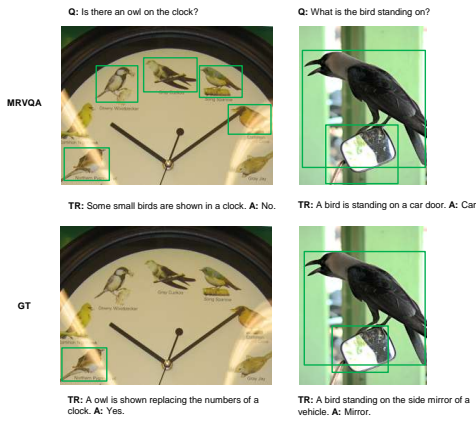


Fig. 6. Two failure cases of our method.

issue may stem from the CLIP model’s strength in capturing global features from large-scale image-caption datasets, which might limit its ability to provide detailed local representations. In the example shown right, although our model accurately understands the cross-modal input and successfully locates the relevant objects, the limited contextual information hampers the precision of the linguistic prediction. The challenge arises because the zoomed-in local view complicates the recognition of the object (e.g., mirror). This scenario emphasizes the importance of a multimodal EVQA model, which provides clear insights compared to a “black box” answering system. Therefore, a promising direction for future work is to explore the usage of models with more advanced feature representations and enhanced cross-modal recognition capabilities, such as ViLBert [24] and BLIP [4].

Moreover, Multimodal Large Language Models (MLLMs) offer a superior approach for cross-modality tasks by leveraging mutual learning. Due to their significantly larger parameter sizes and extensive training datasets, these MLLMs often outperform domain-specific methods. They have gained attention for various vision-language tasks, owing to the capability to deliver high performance through downstream fine-tuning [54], [58]. However, these MLLMs usually respond slowly and demand substantial computational resources for training and fine-tuning. In addition, these models typically generate complex text based on the provided context (e.g., prompt), which may require users to understand or simplify the responses to obtain concise and straightforward answers. In our original intention for this multimodal EVQA task, we try to avoid redundant fine-tuning across multiple predictions while seeking a clean and computation-friendly solution for non-expert users. Recent advancements, such as adaptors (e.g., Lora [59]), significantly reduce the number of trainable parameters in MLLMs. This development facilitates further progress in EVQA research.

## VI. CONCLUSION

In this paper, we propose a multimodal EVQA method that predicts not only answers but also textual and visual rationales to support the answers. To minimize the effort required for annotating precise visual labels, we synthesize a dataset by leveraging existing datasets through a semi-automatic matching and refinement engine. To solve the multimodal EVQA

problem, we introduce MRVQA, a Transformer-based framework that integrates a projection module to align pre-trained features with large language models for generating textual rationales. Additionally, MRVQA employs an open-vocabulary detector to extract precise bounding boxes for consistent visual rationales. Furthermore, to the best of our knowledge, we are the first to propose a metric for evaluating the quality of generated multimodal explanations from a visual perspective. The extensive experiments across four VQA datasets demonstrate that our approach significantly outperforms existing state-of-the-art EVQA methods. We believe these works will inspire further research in the EVQA field.

## REFERENCES

- [1] S. Liu, Z. Zeng, T. Ren, F. Li, H. Zhang, J. Yang, C. Li, J. Yang, H. Su, J. Zhu *et al.*, “Grounding dino: Marrying dino with grounded pre-training for open-set object detection,” *arXiv preprint arXiv:2303.05499*, 2023.
- [2] P. Anderson, X. He, C. Buehler, D. Teney, M. Johnson, S. Gould, and L. Zhang, “Bottom-up and top-down attention for image captioning and visual question answering,” in *Proceedings of the IEEE Conference on Computer Vision and Pattern Recognition*, 2018, pp. 6077–6086.
- [3] R. Dua, S. S. Kancheti, and V. N. Balasubramanian, “Beyond vqa: Generating multi-word answers and rationales to visual questions,” in *Proceedings of the IEEE/CVF Conference on Computer Vision and Pattern Recognition Workshops*, 2021, pp. 1623–1632.
- [4] J. Li, D. Li, C. Xiong, and S. Hoi, “Blip: Bootstrapping language-image pre-training for unified vision-language understanding and generation,” in *International Conference on Machine Learning*, 2022, pp. 12 888–12 900.
- [5] A. Mao, Z. Yang, K. Lin, J. Xuan, and Y.-J. Liu, “Positional attention guided transformer-like architecture for visual question answering,” *IEEE Transactions on Multimedia*, vol. 25, pp. 6997–7009, 2022.
- [6] W. Samek and K.-R. Müller, “Towards explainable artificial intelligence,” *Explainable AI: interpreting, explaining and visualizing deep learning*, pp. 5–22, 2019.
- [7] A. Das, H. Agrawal, L. Zitnick, D. Parikh, and D. Batra, “Human attention in visual question answering: Do humans and deep networks look at the same regions?” *Computer Vision and Image Understanding*, vol. 163, pp. 90–100, 2017.
- [8] D. H. Park, L. A. Hendricks, Z. Akata, A. Rohrbach, B. Schiele, T. Darrell, and M. Rohrbach, “Multimodal explanations: Justifying decisions and pointing to the evidence,” in *Proceedings of the IEEE Conference on Computer Vision and Pattern Recognition*, 2018, pp. 8779–8788.
- [9] Q. Li, Q. Tao, S. Joty, J. Cai, and J. Luo, “Vqa-e: Explaining, elaborating, and enhancing your answers for visual questions,” in *Proceedings of the European Conference on Computer Vision*, 2018, pp. 552–567.
- [10] J. Wu and R. Mooney, “Faithful multimodal explanation for visual question answering,” in *Proceedings of the ACL Workshop BlackboxNLP: Analyzing and Interpreting Neural Networks for NLP*, 2019, pp. 103–112.
- [11] W. Zhang, J. Yu, W. Zhao, and C. Ran, “Dmrfnet: deep multimodal reasoning and fusion for visual question answering and explanation generation,” *Information Fusion*, vol. 72, pp. 70–79, 2021.
- [12] T. Qian, J. Chen, S. Chen, B. Wu, and Y.-G. Jiang, “Scene graph refinement network for visual question answering,” *IEEE Transactions on Multimedia*, vol. 25, pp. 3950–3961, 2022.
- [13] S. Chen and Q. Zhao, “Rex: Reasoning-aware and grounded explanation,” in *Proceedings of the IEEE/CVF Conference on Computer Vision and Pattern Recognition*, 2022, pp. 15 586–15 595.
- [14] K. Papineni, S. Roukos, T. Ward, and W.-J. Zhu, “Bleu: a method for automatic evaluation of machine translation,” in *Proceedings of the 40th annual meeting of the Association for Computational Linguistics*, 2002, pp. 311–318.
- [15] C.-Y. Lin, “Rouge: A package for automatic evaluation of summaries,” in *Text summarization branches out*, 2004, pp. 74–81.
- [16] R. Vedantam, C. Lawrence Zitnick, and D. Parikh, “Cider: Consensus-based image description evaluation,” in *Proceedings of the IEEE Conference on Computer Vision and Pattern Recognition*, 2015, pp. 4566–4575.



- [17] A. Vaswani, N. Shazeer, N. Parmar, J. Uszkoreit, L. Jones, A. N. Gomez, L. u. Kaiser, and I. Polosukhin, "Attention is all you need," in *Advances in Neural Information Processing Systems*, vol. 30, 2017, p. 5998–6008.
- [18] F. Liu, Y. Liu, X. Ren, X. He, and X. Sun, "Aligning visual regions and textual concepts for semantic-grounded image representations," *Advances in Neural Information Processing Systems*, vol. 32, 2019.
- [19] H. Ben-Younes, R. Cadene, M. Cord, and N. Thome, "Mutan: Multimodal tucker fusion for visual question answering," in *Proceedings of the IEEE International Conference on Computer Vision*, 2017, pp. 2612–2620.
- [20] K. Kafle and C. Kanan, "Answer-type prediction for visual question answering," in *Proceedings of the IEEE Conference on Computer Vision and Pattern Recognition*, 2016, pp. 4976–4984.
- [21] T. Qian, R. Cui, J. Chen, P. Peng, X. Guo, and Y.-G. Jiang, "Locate before answering: Answer guided question localization for video question answering," *IEEE Transactions on Multimedia*, 2023.
- [22] K. Li, G. Vosselman, and M. Y. Yang, "Hrvqa: A visual question answering benchmark for high-resolution aerial images," *ISPRS Journal of Photogrammetry and Remote Sensing*, vol. 214, pp. 65–81, 2024.
- [23] Z. Yu, J. Yu, Y. Cui, D. Tao, and Q. Tian, "Deep modular co-attention networks for visual question answering," in *Proceedings of the IEEE/CVF Conference on Computer Vision and Pattern Recognition*, 2019, pp. 6281–6290.
- [24] J. Lu, D. Batra, D. Parikh, and S. Lee, "Vilbert: Pretraining task-agnostic visiolinguistic representations for vision-and-language tasks," *Advances in Neural Information Processing Systems*, vol. 32, 2019.
- [25] L. Zhou, H. Palangi, L. Zhang, H. Hu, J. Corso, and J. Gao, "Unified vision-language pre-training for image captioning and vqa," in *Proceedings of the AAAI Conference on Artificial Intelligence*, vol. 34, 2020, pp. 13 041–13 049.
- [26] R. Zellers, Y. Bisk, A. Farhadi, and Y. Choi, "From recognition to cognition: Visual commonsense reasoning," in *Proceedings of the IEEE/CVF Conference on Computer Vision and Pattern Recognition*, 2019, pp. 6720–6731.
- [27] D. A. Hudson and C. D. Manning, "Gqa: A new dataset for real-world visual reasoning and compositional question answering," in *Proceedings of the IEEE/CVF Conference on Computer Vision and Pattern Recognition*, 2019, pp. 6700–6709.
- [28] C. Chen, S. Anjum, and D. Gurari, "Grounding answers for visual questions asked by visually impaired people," in *Proceedings of the IEEE/CVF Conference on Computer Vision and Pattern Recognition*, 2022, pp. 19 098–19 107.
- [29] S. Hochreiter and J. Schmidhuber, "Long short-term memory," *Neural computation*, vol. 9, no. 8, pp. 1735–1780, 1997.
- [30] A. Marasović, C. Bhagavatula, J. S. Park, R. Le Bras, N. A. Smith, and Y. Choi, "Natural language rationales with full-stack visual reasoning: From pixels to semantic frames to commonsense graphs," in *Findings of the Association for Computational Linguistics: EMNLP*, 2020, pp. 2810–2829.
- [31] D. Xue, S. Qian, and C. Xu, "Variational causal inference network for explanatory visual question answering," in *Proceedings of the IEEE/CVF International Conference on Computer Vision*, 2023, pp. 2515–2525.
- [32] A. Fukui, D. H. Park, D. Yang, A. Rohrbach, T. Darrell, and M. Rohrbach, "Multimodal compact bilinear pooling for visual question answering and visual grounding," in *Proceedings of the Conference on Empirical Methods in Natural Language Processing*, 2016, pp. 457–468.
- [33] L. Xiao, X. Yang, F. Peng, M. Yan, Y. Wang, and C. Xu, "Clip-vg: Self-paced curriculum adapting of clip for visual grounding," *IEEE Transactions on Multimedia*, 2023.
- [34] C. Deng, Q. Wu, Q. Wu, F. Hu, F. Lyu, and M. Tan, "Visual grounding via accumulated attention," in *Proceedings of the IEEE Conference on Computer Vision and Pattern Recognition*, 2018, pp. 7746–7755.
- [35] Z. Yang, B. Gong, L. Wang, W. Huang, D. Yu, and J. Luo, "A fast and accurate one-stage approach to visual grounding," in *Proceedings of the IEEE/CVF International Conference on Computer Vision*, 2019, pp. 4683–4693.
- [36] A. Chandrasekaran, V. Prabhu, D. Yadav, P. Chattopadhyay, and D. Parikh, "Do explanations make vqa models more predictable to a human?" in *Proceedings of the Conference on Empirical Methods in Natural Language Processing*, 2018, pp. 1036–1042.
- [37] T.-Y. Lin, M. Maire, S. Belongie, J. Hays, P. Perona, D. Ramanan, P. Dollár, and C. L. Zitnick, "Microsoft coco: Common objects in context," in *European Conference on Computer Vision*, 2014, pp. 740–755.
- [38] A. Radford, J. W. Kim, C. Hallacy, A. Ramesh, G. Goh, S. Agarwal, G. Sastry, A. Askell, P. Mishkin, J. Clark *et al.*, "Learning transferable visual models from natural language supervision," in *International Conference on Machine Learning*, 2021, pp. 8748–8763.
- [39] A. Dosovitskiy, L. Beyer, A. Kolesnikov, D. Weissenborn, X. Zhai, T. Unterthiner, M. Dehghani, M. Minderer, G. Heigold, S. Gelly *et al.*, "An image is worth 16x16 words: Transformers for image recognition at scale," *arXiv preprint arXiv:2010.11929*, 2020.
- [40] T. Darcet, M. Oquab, J. Mairal, and P. Bojanowski, "Vision transformers need registers," in *International Conference on Learning Representations*, 2024.
- [41] A. Radford, J. Wu, R. Child, D. Luan, D. Amodei, I. Sutskever *et al.*, "Language models are unsupervised multitask learners," *OpenAI blog*, vol. 1, no. 8, p. 9, 2019.
- [42] D. Teney, P. Anderson, X. He, and A. Van Den Hengel, "Tips and tricks for visual question answering: Learnings from the 2017 challenge," in *Proceedings of the IEEE Conference on Computer Vision and Pattern Recognition*, 2018, pp. 4223–4232.
- [43] P. Anderson, B. Fernando, M. Johnson, and S. Gould, "Spice: Semantic propositional image caption evaluation," in *Proceedings of the European Conference on Computer Vision*, 2016, pp. 382–398.
- [44] Z. Li, X. Zhang, Y. Zhang, D. Long, P. Xie, and M. Zhang, "Towards general text embeddings with multi-stage contrastive learning," *arXiv preprint arXiv:2308.03281*, 2023.
- [45] M. Everingham, L. Van Gool, C. K. Williams, J. Winn, and A. Zisserman, "The pascal visual object classes (voc) challenge," *International Journal of Computer Vision*, vol. 88, pp. 303–338, 2010.
- [46] Y. Goyal, T. Khot, D. Summers-Stay, D. Batra, and D. Parikh, "Making the v in vqa matter: Elevating the role of image understanding in visual question answering," in *Proceedings of the IEEE conference on computer vision and pattern recognition*, 2017, pp. 6904–6913.
- [47] B. Patro, S. Patel, and V. Nambodiri, "Robust explanations for visual question answering," in *Proceedings of the IEEE/CVF Winter Conference on Applications of Computer Vision*, 2020, pp. 1577–1586.
- [48] P. Wang, A. Yang, R. Men, J. Lin, S. Bai, Z. Li, J. Ma, C. Zhou, J. Zhou, and H. Yang, "Ofa: Unifying architectures, tasks, and modalities through a simple sequence-to-sequence learning framework," in *International Conference on Machine Learning*, 2022, pp. 23 318–23 340.
- [49] D. P. Kingma and J. Ba, "Adam: A method for stochastic optimization," *arXiv preprint arXiv:1412.6980*, 2014.
- [50] S. Banerjee and A. Lavie, "Meteor: An automatic metric for mt evaluation with improved correlation with human judgments," in *Proceedings of the ACL Workshop on Intrinsic and Extrinsic Evaluation Measures for Machine Translation and/or Summarization*, 2005, pp. 65–72.
- [51] H. Tan and M. Bansal, "Lxmert: Learning cross-modality encoder representations from transformers," in *Proceedings of the Conference on Empirical Methods in Natural Language Processing*, 2019, pp. 5100–5111.
- [52] Y.-C. Chen, L. Li, L. Yu, A. El Kholy, F. Ahmed, Z. Gan, Y. Cheng, and J. Liu, "Uniter: Universal image-text representation learning," in *European conference on computer vision*, 2020, pp. 104–120.
- [53] S. Li, C. Gong, Y. Zhu, C. Luo, Y. Hong, and X. Lv, "Context-aware multi-level question embedding fusion for visual question answering," *Information Fusion*, vol. 102, p. 102000, 2024.
- [54] J. Li, D. Li, S. Savarese, and S. Hoi, "Blip-2: Bootstrapping language-image pre-training with frozen image encoders and large language models," in *International Conference on Machine Learning*, 2023, pp. 19 730–19 742.
- [55] C. Li, "Large multimodal models: Notes on cvpr 2023 tutorial," *arXiv preprint arXiv:2306.14895*, 2023.
- [56] T. Brown, B. Mann, N. Ryder, M. Subbiah, J. D. Kaplan, P. Dhariwal, A. Neelakantan, P. Shyam, G. Sastry, A. Askell *et al.*, "Language models are few-shot learners," *Advances in Neural Information Processing Systems*, vol. 33, pp. 1877–1901, 2020.
- [57] L. H. Li, P. Zhang, H. Zhang, J. Yang, C. Li, Y. Zhong, L. Wang, L. Yuan, L. Zhang, J.-N. Hwang *et al.*, "Grounded language-image pre-training," in *Proceedings of the IEEE/CVF Conference on Computer Vision and Pattern Recognition*, 2022, pp. 10 965–10 975.
- [58] Z. Peng, W. Wang, L. Dong, Y. Hao, S. Huang, S. Ma, and F. Wei, "Kosmos-2: Grounding multimodal large language models to the world," *arXiv preprint arXiv:2306.14824*, 2023.
- [59] E. J. Hu, Y. Shen, P. Wallis, Z. Allen-Zhu, Y. Li, S. Wang, L. Wang, and W. Chen, "Lora: Low-rank adaptation of large language models," *arXiv preprint arXiv:2106.09685*, 2021.